

Interannual Variability in Weddell Sea Ice Formation and Bottom Water Outflow in response to the Antarctic Circumpolar Wave

Drinkwater, M.R

Jet Propulsion Laboratory,
California Institute of Technology
4800 Oak Grove Drive,
Pasadena, CA 91109, USA
(818) 3936720
mrd@pacific.jpl.nasa.gov

Kreyscher, M.

Alfred Wegener Institut
für Polar und Meeresforschung
Haus C, Physik I
Am Handelshafen 12,
D-27570 Bremerhaven, Germany
mkreysch@awi-bremerhaven.de

The seasonal sea-ice cover surrounding the continent of Antarctica, together with the circumpolar current belt, form a contiguous pathway for propagation and transfer of climatological anomalies around the Southern hemisphere. Recent discovery of a clockwise (eastward) propagating pattern of interlocking positive and negative atmospheric and oceanographic anomalies, led to the origin of the term “Antarctic Circumpolar Wave” (ACW) [White and Peterson, 1996]. Sea ice is found to react markedly to the ACW on interannual timescales, with expression of anomalies in its extent. In this study, further reactions ice the Weddell Sea ice cover to climatological anomalies are discussed, including both its dynamic-thermodynamic response to wind forcing, and particularly interannual variability in ice production induced by the ACW.

This study combines Weddell Sea measurement records obtained from satellite and oceanographic sensors and compares them with simulation data from a dynamic-thermodynamic sea-ice model. Results demonstrate demonstrates that there is significant interannual variability in observed sea-ice extent, sea-surface temperature, sea-level pressure, and open-water fraction, together with simulated net-freezing rate, over the period 1986-1992. Interannual variability of these regional parameters is phase-locked to a propagating series of coupled anomalies, observed and characterised as the ACW. Coincident German measurements of Weddell Sea bottom water outflow [Fahrbach *et al.*, 1995] indicate pronounced interannual variability which appears linked to ACW forcing. The proposed explanation is dynamically-driven opening of the ice-shelf polynya system in the south-western Weddell Sea, during periods with higher than normal meridional wind stresses. Enhanced production of open water has a direct impact on simulated net ice production in the study region. It is suggested that salt rejection during ice formation, in this western shelf location, contributes significantly to production of the dense

“
water which recent tracer studies have shown to be the main “source” component in bottom water exiting the **Weddell** Sea basin at **Joinville** Island [**Weppernig** *et al.*, 1996].

These results provide a clearer understanding of the communication between polar ocean and atmosphere in the context of seasonal to interannual variability in sea-ice growth and **water-mass** production. They highlight the potential control of **interannual** variations in net winter regional sea-ice formation upon bottom-water outflow. Moreover, they indicate that Antarctic sea-ice cover participates actively in transmitting climate anomalies. This raises the question as to whether the resulting **timescales** of variability in bottom water outflow can have significant impact on the global **thermohaline** circulation and the “climate” of the world ocean.

This work was conducted at Jet Propulsion Laboratory, California Institute of Technology, under contract to NASA. Funding support was provided by Robert Thomas (Code YSG) in the NASA Office for Mission to Planet Earth.

Interannual Variability in Weddell Sea Ice Formation and Bottom Water Outflow in response to the Antarctic Circumpolar Wave

Drinkwater, M.R

Jet Propulsion Laboratory,
California Institute of Technology
4800 Oak Grove Drive,
Pasadena, CA 91109, USA
(818) 3936720
mrd@pacific.jpl.nasa.gov

Kreyscher, M.

Alfred Wegener Institut
für Polar und Meeresforschung
Haus C, Physik I
Am Handelshafen 12,
D-27570 Bremerhaven, Germany
mkreysch@awi-bremerhaven.de

The seasonal sea-ice cover surrounding the continent of Antarctica, together with the circumpolar current belt, form a contiguous pathway for propagation and transfer of climatological anomalies around the Southern hemisphere. Recent discovery of a clockwise (eastward) propagating pattern of interlocking positive and negative atmospheric and oceanographic anomalies, led to the origin of the term “Antarctic Circumpolar Wave” (ACW) [White and Peterson, 1996]. Sea ice is found to react markedly to the ACW on interannual timescales, with expression of anomalies in its extent. In this study, further reactions of the Weddell Sea ice cover to climatological anomalies are discussed, including both its dynamic-thermodynamic response to wind forcing, and particularly interannual variability in ice production induced by the ACW.

This study combines Weddell Sea measurement records obtained from satellite and oceanographic sensors and compares them with simulation data from a dynamic-thermodynamic sea-ice model. Results demonstrate that there is significant interannual variability in observed sea-ice extent, sea-surface temperature, sea-level pressure, and open-water fraction, together with simulated net-freezing rate, over the period 1986-1992. Interannual variability of these regional parameters is phase-locked to a propagating series of coupled anomalies, observed and characterised as the ACW. Coincident German measurements of Weddell Sea bottom water outflow [Fahrbach *et al.*, 1995] indicate pronounced interannual variability which appears linked to ACW forcing. The proposed explanation is dynamically-driven opening of the ice-shelf polynya system in the south-western Weddell Sea, during periods with higher than normal meridional wind stresses. Enhanced production of open water has a direct impact on simulated net ice production in the study region. It is suggested that salt rejection during ice formation, in this western shelf location, contributes significantly to production of the dense

water which recent tracer studies have shown to be the main “source” component in bottom water exiting the **Weddell** Sea basin at **Joinville** Island [Weppernig *et al.*, 1996].

These results provide a clearer understanding of the communication between polar ocean and atmosphere in the context of seasonal to **interannual** variability in sea-ice growth and **water-mass** production. They highlight the potential control of **interannual** variations in net winter regional sea-ice formation upon bottom-water outflow. Moreover, they indicate that Antarctic sea-ice cover participates actively in transmitting climate anomalies. This raises the question as to whether the resulting **timescales** of variability in bottom water outflow can have significant impact on the global **thermohaline** circulation and the “climate” of the world ocean.

This work was conducted at Jet Propulsion Laboratory, California Institute of Technology, under contract to NASA. Funding support was provided by Robert Thomas (Code YSG) in the NASA Office for Mission to Planet Earth.

Hybrid Concatenated Codes and Iterative Decoding

Dariusz Divsalar and Fabrizio Pollara¹

Jet Propulsion Laboratory, California Institute of Technology
4800 Oak Grove Drive, Pasadena, CA 91109-8099
E-mail: dariush@shannon.jpl.nasa.gov

Abstract — A hybrid concatenated code is a combination of parallel and serial concatenated codes. Here we consider an example with three codes and two interleaves. An upper bound to the bit error rate (BER) of the hybrid code is obtained. Design rules for the three component codes that maximize the interleaves gain and the asymptotic slope of the BER curves are discussed. A low-complexity iterative decoding algorithm with near maximum-likelihood performance is proposed. Comparisons with “turbo codes” and with serially concatenated codes show that the hybrid scheme offers better performance at very low BER.

I. INTRODUCTION

Turbo codes are *parallel* concatenated convolutional codes with two [1] or more constituent codes. *Serially* concatenated convolutional codes have been shown to yield performance comparable, and in some cases superior, to turbo codes. A third choice is a *hybrid* concatenation of convolutional codes (HCCC). Here we only consider, as an example of HCCC, the structure shown in Fig. 1. The (suboptimum) decoding process is based on iterating a soft-input soft-output a-posteriori probability module, applied to each constituent code.

II. PERFORMANCE BOUNDS FOR HCCCS

The example of hybrid structure shown in Fig. 1 includes a *parallel* convolutional code C_p with rate $R_c^p = k/n_1$ and equivalent block code representation $(N_1/R_c^p, N_1)$, an *outer* $(N_1/R_c^o, N_1)$ code C_o with rate $R_c^o = k/p$, an *inner* $(N_2/R_c^i, N_2)$ code C_i with rate $R_c^i = p/n_2$, plus a N_1 -bit and a N_2 -bit interleave. This gives an HCCC with overall rate $R_c = k/(n_1 + n_2)$.

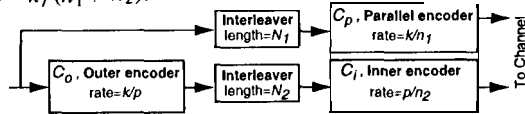


Figure 1: A hybrid concatenated code.

Using analytical tools and notation introduced in [2], we obtained the following bound on BER, averaged over all possible permutations,

$$P_b(e) \leq \sum_{h_1=h_m^p}^{N_1/R_c^p} \sum_{h_2=h_m^i}^{N_2/R_c^i} \sum_{w=w_m}^{N_1} \sum_{e=0}^{N_2} \frac{w A_{w,h_1}^{C_p} A_{w,e}^{C_o} A_{e,h_2}^{C_i}}{N_1 \binom{N_1}{w} \binom{N_2}{e}} e^{-(h_1+h_2)R_c E_b/N_o},$$

where w_m is the minimum input weight for error events of C_p and C_o , h_m^p and h_m^i are the minimum weights of the codewords of C_p and C_i respectively, E_b/N_o is the signal-to-noise ratio per bit, $A_{w,e}^{C_o}$ is the number of codewords of C_o of weight e given by with input sequences of weight w . Analogous definitions apply for $A_{w,h_1}^{C_p}$ and $A_{e,h_2}^{C_i}$. We have computed the bound for a specific rate 1/4 HCCC formed by a 4-state C_p (recursive, systematic, $R_c^p = 1/2$), where, as in “turbo codes”, the systematic bits are not transmitted, a 4-state C_o (nonrecursive, $R_c^o = 1/2$), and a 4-state C_i (recursive, systematic, $R_c^i = 2/3$), joined by two interleaves of lengths $N_1 = N$ and $N_2 = 2N$. The respective generator matrices are $\begin{bmatrix} 1 & \\ & 1+D^2 \end{bmatrix}$, $\begin{bmatrix} 1+D & \\ & 1+D^2 \end{bmatrix}$ and

$\begin{bmatrix} 1 & 0 & (1+D^2)/(1+D+D^2) \\ 0 & 1 & (1+D)/(1+D+D^2) \end{bmatrix}$. The BER performance bounds show a very significant interleaving gain (IG), i.e., lower values of BER for higher values of N . At $E_b/N_o = 3$ dB, BER is 3×10^{-5} , 8×10^{-7} , 4×10^{-9} , 10^{-10} , and 2×10^{-11} , for $N = 20, 40, 100, 200, 300$, respectively. Simulation of the proposed iterative decoder produced $\text{BER} = 10^{-7}$ at $E_b/N_o = 0.2$ dB, with 15 iterations and $N = 16384$.

III. DESIGN OF HCCCS

Two quantities are important in the asymptotic behavior of the bound inequality above: The exponent of N for minimum output weight, $\alpha(h_1, h_2)$, and the maximum exponent of N , $\alpha_M = \max_{h_1, h_2} \{\alpha(h_1, h_2)\}$ with the corresponding output weight, where $N \triangleq N_2/p = N_1/k$. For large values of E_b/N_o , the performance of the HCCC is dominated by the first terms of the summations in h_1 and h_2 , corresponding to the minimum values $h_1 = h_m^p$, and $h_2 = h_m^i$. If C_p is nonrecursive, we have $\alpha(h_m^p, h_m^i) \leq 1 - d_f^o$, where d_f^o is the minimum Hamming distance of C_o , which is reminiscent of serial concatenation. If C_p is recursive, we have $\alpha(h_m^p, h_m^i) \leq -d_f^o$, i.e., the exponent of N corresponding to minimum weight codewords is always negative, thus yielding IG at high E_b/N_o . This suggests that, for values of E_b/N_o and N where the HCCC performance is dominated by its free distance? $= h_m^p + h_m^i$, increasing the interleave length yields a gain in performance. To increase IG, one should choose a recursive encoder for C_p , and a C_o with large d_f^o . To improve the performance with E_b/N_o , one should choose a $\{C_i, C_p\}$ combination such that $h_m^p + h_m^i$ is large. However, as in serial concatenated codes there are coefficients of the exponents in h_1 , and h_2 for $h_1 > h_m^p$, and $h_2 > h_m^i$ that increase with N . To investigate this phenomenon we evaluate α_M , which allows us to find the dominant contribution to BER for $N \rightarrow \infty$. If C_i is nonrecursive, and C_p or C_o are nonrecursive then we have $\alpha_M \geq 0$, and IG is not allowed, If C_i is nonrecursive, and both C_p and C_o are recursive then we have $\alpha_M = -1$, and IG is allowed, as for “turbo codes”. If C_i is recursive, and C_p is nonrecursive we have $\alpha_M \leq -\lfloor (d_f^o + 1)/2 \rfloor$, and IG is allowed, as in serial concatenated codes. If C_i is recursive, and C_p is recursive we have $\alpha_M \leq -\lfloor (d_f^o + 3)/2 \rfloor$, and IG is higher than for serial concatenated codes. Based on the above analysis, in order to achieve the highest IG in HCCCS, we should select the component codes as follows: a recursive C_i ; a recursive C_p ; C_o can be either nonrecursive or recursive but should have large d_f^o . Next we consider the weight $h(\alpha_M)$ which is the sum of output weights of C_i and C_p associated to the highest exponent of N . We have $h(\alpha_M) = d_f^o d_{\text{eff}}^i / 2 + d_{\text{eff}}^p$, for d_f^o even, and $h(\alpha_M) = (d_f^o - 3) d_{\text{eff}}^i / 2 + h_m^{(3)} + d_{\text{eff}}^p$, for d_f^o odd, where $h_m^{(3)}$ is the minimum weight of codewords of C_i generated by a weight 3 input sequence, and d_{eff}^i , and d_{eff}^p are the effective free distances of C_i and C_p .

REFERENCES

- [1] C. Berrou, A. Glavieux, and P. Thitimajshima, “Near Shannon Limit Error-Correcting Coding and Decoding: Turbo-Codes”, *Proc. of ICC '93*, Geneva, May 1993, pp. 1064-1070.
- [2] S. Benedetto and G. Montorsi, “Unveiling turbo-codes: some results on parallel concatenated coding schemes”, *IEEE Trans. on Information Theory*, vol. 43, no. 2, Mar. 1996.

¹This research was carried out at the Jet Propulsion Laboratory, California Institute of Technology, under a contract with NASA.